

# Kilpisjärvi Atmospheric Imaging Receiver Array – First Results

Juha Vierinen  
MIT Haystack Observatory  
Westford, MA 01886  
Email: x@mit.edu

Derek McKay-Bukowski  
Markku S. Lehtinen  
Antti Kero  
Thomas Ulich  
Sodankylä Geophysical Observatory  
Tähteläntie 62, 99600  
Sodankylä, Finland.  
Email: derek@sgo.fi

**Abstract**—The Kilpisjärvi Atmospheric Imaging Receiver Array (KAIRA) is a dual antenna array radio receiver based on LOFAR technology. The main purpose of the system is to function as a bi-static phased-array receiver for the EISCAT Tromsø VHF incoherent scatter radar, as well as to function as a wide band imaging riometer. Due to the wide frequency coverage, the system can also be used as a bi-static radar receiver for various nearby meteor- and MST-radars. Other examples of possible uses for the system include broad-band observations of solar radio emissions and ionospheric scintillation. In addition to a technical overview, we present the first results from this recently completed system. These include the first multi-beam bi-static incoherent scatter radar observation, as well as a broad-band riometer absorption measurement.

## I. INTRODUCTION

The Low Frequency Array (LOFAR) is a radio telescope network intended for low frequency astronomy [1]. Due to nature of low-frequency radio propagation [2], spatiotemporally variable ionospheric effects have to be routinely estimated in the process of producing very long baseline radio images. Because the radio frequencies covered by the LOFAR stations experience ionospheric effects, such as ionospheric delays, Faraday-rotation and absorption, it is natural to also consider using these measurements for ionospheric remote sensing. The wide frequency coverage also allows the radio telescope to function as a radar receiver for several different types of radars.

The main goal for building the Kilpisjärvi Atmospheric Imaging Receiver Array (KAIRA) was to use a LOFAR-based system as a bi-static phased-array radar receiver for the EISCAT VHF [3] incoherent scatter radar transmitter in Norway. This receiver was to act as a pathfinder for the planned EISCAT3D [4] radar. The purpose was to demonstrate that incoherent scatter radar measurements could be successfully performed with modern wide-band phased-array radio telescope technology. A secondary goal was to demonstrate that the technology can be multi-use, i.e., that the same radio telescope could also be used for a large number of other active and passive geophysical remote-sensing experiments, which are typically not possible with traditional incoherent scatter radars, due to their inherent narrow-band nature.

In this paper, we will go through the technical specifications of KAIRA and give an overview of some of the first

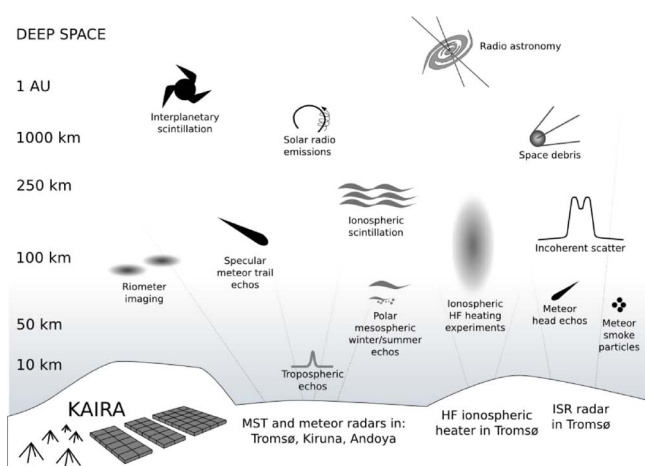


Fig. 1. Figurative overview of the main science objectives of KAIRA. Of these, incoherent scatter radar and wide band imaging riometry plays the main role.

results obtained using the system in its commissioning phase. We will also discuss the planned future use of the instrument.

## II. IMPLEMENTATION

### A. Site selection and preparation

A Finnish site was chosen in 2009 at a favourable distance from the EISCAT radar facility at Ramfjordmoen, near Tromsø, permitting a suitable observing angle for bi-static incoherent scatter measurements ( $\sim 45^\circ$  at 80–100 km altitude above the transmitter). Stable, elevated ground was chosen to protect against permafrost shifting and to provide a wind-shear effect over the site in order to assist in the natural clearing of snow. Following an initial winter-test of hardware, construction took place during the summers of 2010 and 2011. The stations became operational in September 2012 and shall operate for at least one complete solar cycle.

KAIRA comprises two 48-element, dual-polarisation arrays: the High-Band Antenna (HBA) array and Low-Band Antenna (LBA) array. Each HBA is a ‘tile’ containing 16 crossed-bowtie elements, integrated ground plane and a remotely controlled analogue first-stage beamformer. The tiles

TABLE I. PARAMETERS FOR THE TWO KAIRA ARRAYS. COORDINATES ARE IN ETRS89/EUREF-FIN. THE GEOGRAPHIC HEIGHT REFERENCE SYSTEM FOR BOTH GK/N60 AND GRS IS GIVEN. LONGITUDE AND LATITUDE ARE IN DEGREES; ALL OTHERS ARE IN METRES.

Parameter	LBA Array	HBA Array
Num. antennas	48	48
Antenna type	inverted-V dipoles	16-element tiles
Polarisations	2	2
Array layout	sparse, quasi-random	segmented rectangular
Array physical size	~34 m diameter	30 x 50 m
Array alignment	symmetrical	313.95 degrees
Min. frequency	10 MHz	110 MHz
Max. frequency	80 MHz	270 MHz
RCU modes	RCU-3 & 4	RCU-5, 6 & RCU-7
Beam-forming	digital	analogue in each tile; digital over array
Longitude	20.76207580 E	20.76103311 E
Latitude	69.07074450 N	69.07105610 N
Height (GK)	493.123	495.086
Height (GRS)	523.371	525.336
Geocentric-X	2136833.225	2136818.264
Geocentric-Y	810088.740	810038.592
Geocentric-Z	5935285.279	5935299.531

are mounted on “framesets” — open timber latices which stand 1.5 m above ground — to provide additional defence against snow. These 16×48 antenna elements are arranged in a semi-regular grid. Each LBA is a crossed inverted-V-dipole aerial, standing 1.8 m tall above a 3 m by 3 m steel ground plane. The LBAs are scattered in a quasi-random pattern across a field 34 metres in diameter to give a good beam-profile with low sidelobes. Coaxial cable connects each antenna to an industry-standard shipping container fitted with an RF-shielded enclosure to act as a Faraday cage, thus preventing the enclosed electronics interfering with the arrays.

The coordinates for the centres of the two arrays are given in Table I.

### B. Signal and data processing

KAIRA uses the standard LOFAR signal processing system described in [5]. There are 96 receiver unit (RCU) boards (1 per HBA/LBA pair) processing the 48×2 polarisations. Each RCU has switches and filters to independently select the required antenna input and observing frequency band for each channel; the selection combination is referred to as the ‘RCU mode’. Sampling may be done at either 200 or 160 MHz using either 12-, 8- or 4-bit analogue-to-digital conversion.

The entire LBA and HBA arrays cannot be used simultaneously, but combinations of subsets of antennas can be selected to permit observations across the entire frequency capability of the system, albeit with a trade-off in sensitivity and resolution.

The RCU modes are listed in Table II. In September 2012, KAIRA became the first LOFAR-based facility to operate the three most common modes simultaneously — the so-called ‘mode 357’.

After digitisation, the signal is split into 512 ‘subbands’ via a polyphase filter and 1024-point fast Fourier transform. The subbands, each from an arbitrary set of antennas, can be arbitrarily selected and combined into ‘beamlets’ using a complex-weighted, phase-rotated beamformer. This allows for trade-offs between antennas, bandwidth ( $\Delta\nu$ ), number of

TABLE II. STATION RECEIVER (RCU) MODES. IN MODE 5, THE NOMINAL RECEIVER BAND IS INVERTED (CORRECTED LATER IN THE PROCESSING CHAIN). MODE 0 IS USED TO DISABLE AN RCU WITHIN THE CURRENT OBSERVATION. MODES 1 AND 2 ARE UNUSED AT THIS STAGE.

Mode	RCU input	Nyquist zone	Receiver band (MHz)	Approx. actual passband (MHz)
0	—	—	—	—
1	LBL	I	0–100	8–80
2	LBL	I	0–100	28–80
3	LBH	I	0–100	8–80
4	LBH	I	0–100	28–80
5	HBA	II	200–100	110–191
6	HBA	III	160–240	165–235
7	HBA	III	200–300	209–270

TABLE III. SIGNAL-PROCESSING PARAMETERS FOR THE KAIRA FACILITY. THE THREE COLUMNS REFLECT DIFFERENCES WHEN SELECTING DIFFERENT NUMBERS OF SAMPLE BITS.

Parameter	Performance		
Subbands per RCU	512	512	512
Sample bit depth	12	8	4
Num. simultaneous beams	244	488	976
Polarisations per beam	2	2	2
Cumulative $\Delta\nu$ (200 MHz)	47.7	95.3	190.6 MHz
Cumulative $\Delta\nu$ (160 MHz)	38.1	76.3	152.5 MHz
Spectral Resolution (200 MHz)	195.31	195.31	195.31 kHz
Spectral Resolution (160 MHz)	156.25	156.25	156.25 kHz

beamlets and bits of digitisation. These system parameters are summarised in Table III.

Because beam-forming takes place after the digitisation of the signal, it permits rapid re-pointing of the array as well as simultaneous observation in multiple directions. In addition to beamformed data products, a local correlator records visibilities between antennas. An automated control system permits remote operation with no local human presence.

## III. SCIENCE

The main science topics that are addressed by KAIRA are depicted in Figure 1. These include wide band imaging riometry, interplanetary scintillation [6], [7], solar radio emission studies [8], ionospheric scintillation [9], multi-static micrometeor head echo trajectory measurements [10], active ionospheric modification measurements using HF heating [11], [12], [13], multistatic, multi-frequency measurements of polar mesospheric winter and summer echoes [14], and wide-band imaging riometer. Due to the flexibility of the underlying technology, there are many other possible types of experiments and it is possible that many more new innovative experiments will be conceived in the future.

While the main use of the system is not radio astronomy, we also intend to occasionally use the system for astronomical measurements, as KAIRA can be used to significantly increase the longest baseline of the LOFAR VLBI network.

During the commissioning stage of the radio telescope, we have so far demonstrated successful measurements of incoherent scatter radar, riometer absorption, ionospheric scintillation, and very long baseline interferometric fringes.

### A. Incoherent scatter radar

Multi-static incoherent scatter radar measurement capability offers the possibility of measuring instantaneously a

full profile of vector velocities, which can be used to, e.g., derive ionospheric neutral winds and electric fields [15]. The asymmetry of the plasma-line can also yield useful information about electron temperature (see [16] and references therein).

A phased-array radio receiver capable of simultaneously forming multiple beams also has the advantage the receiver can be used to observe different altitudes illuminated by the transmitter, allowing bi-static measurements of the full altitude profile – something that is not possible using conventional parabolic dishes.

To demonstrate that KAIRA can be used for incoherent scatter radar measurements, on 21 August 2012, we performed a bi-static incoherent radar experiment together with the EISCAT VHF radar in Ramfjordmoen, approximately 85 km northwest from KAIRA. In this experiment, we transmitted a optimised code group [17] of 20 codes with 128  $\mu$ s baud lengths and 10 bits per code. Figure 2 shows the lag-profile inversion [18] result of a 512-second integration period. The time-delay between the transmitter and the receiver is given in round-trip propagation time with light propagation distance in kilometres  $R = (t \cdot c)/(2 \cdot 10^3)$ , where  $t$  is the time delay between Tromsø and KAIRA. During the experiment we had 30 dual polarised beams intersecting the Tromsø VHF vertical beam at altitudes between 90 km and 2000 km. In this plot, we have combined all polarisations and beams simply by averaging the autocorrelation functions together. This is not the most optimal way of combining the polarisations and beams, and improving this is a topic of future work.

During the first measurement, we also observed a large number of echoes associated with space objects and meteor head echos. We also observed echoes that probably originate from ground or tropospheric propagation from the EISCAT VHF transmitter.

### B. Wide band riometer

A LOFAR LBA covers the range of frequencies approximately between 10 and 80 MHz. This is a range of frequencies that are typically used for riometers [19]. Thus, the LOFAR LBA can be used to measure the absorption of cosmic radio waves in the D-region of the ionosphere. This can be used to, e.g., estimate the electron density or the electron neutral collision frequency [20]. The novel feature enabled by the use of LOFAR technology is that it can measure the continuum of frequencies in the 10-80 MHz, instead of one or a few narrow frequencies. This allows significantly better statistics, tolerance to radio interference and, perhaps most importantly, this allows us to measure the frequency dependence of the absorption, which in turn can be used to estimate the electron density profile of the D-region [21].

Because the EISCAT VHF system is not transmitting for most of the time, KAIRA usually operates in imaging riometer mode. This will allow us to construct a long statistical record of auroral precipitation effects in the mesosphere. The first high-energy precipitation event observed using KAIRA was obtained on 13 November 2012. At this point we only had one beam measuring towards zenith. The measured frequency and time-dependent absorption is shown in Fig. 3. The plot starts at 12:00 UTC. Strong absorption features can be seen in the plot a after midnight. This is associated with auroral

precipitation. Parts of the daytime spectrum are contaminated with radio broadcasts but, even then, it is possible to see the behaviour of the background cosmic noise between the bands of interference. Also, the approximately  $1/f^2$  dependence of the riometer absorption can be seen in the figure too.

## IV. CONCLUSIONS AND FUTURE WORK

We have demonstrated that it is possible to use the LOFAR digital phased-array radio telescope technology as a bi-static incoherent scatter radar receiver, as well as a wide-band riometer.

While we only present some of the first results in this paper, we have already successfully performed several other measurements that address the many of the other science goals shown in Fig. 1, and we are currently working towards publishing these results.

## ACKNOWLEDGEMENTS

The authors would like to thank all the people that helped build KAIRA. The work has been supported by the Academy of Finland (Finnish Programme for Centres of Excellence in Research 2006-2013). The EISCAT measurements were made with publicly accessible measurements. EISCAT is an international association supported by China (CRIRP), Finland (SA), Germany (DFG), Japan (STEL and NIPR), Norway (NFR), Sweden (VR) and United Kingdom (STFC).

## REFERENCES

- [1] M.P. van Haarlem et al., “LOFAR: The LOw-Frequency ARray,” *ArXiv e-prints*, May 2013.
- [2] K. Budden, *The Propagation of Radio Waves: The Theory of Radio Waves of Low Power in the Ionosphere and Magnetosphere*. Cambridge University Press, 1988.
- [3] M. Baron, “EISCAT progress 1983-1985,” *Journal of Atmospheric and Terrestrial Physics*, vol. 48, no. 9-10, pp. 767–772, 1986.
- [4] “EISCAT3D FP6 Design Study Summary,” 2009.
- [5] M. de Vos, A. W. Gunst, and R. Nijboer, “The LOFAR Telescope: System Architecture and Signal Processing,” *IEEE Proceedings*, vol. 97, pp. 1431–1437, Aug. 2009.
- [6] A. Hewish, P. F. Scott, and D. Wills, “Interplanetary Scintillation of Small Diameter Radio Sources,” *Nature*, vol. 203, pp. 1214–1217, Sep. 1964.
- [7] D. Oberoi and J. Kasper, “LOFAR: The potential for solar and space weather studies,” *Planetary and Space Science*, vol. 52, no. 15, pp. 1415 – 1421, 2004.
- [8] J.-P. Raulin and A. A. Pacini, “Solar radio emissions,” *Advances in Space Research*, vol. 35, pp. 739–754, 2005.
- [9] N. Meyer-Vernet, G. Daigne, and A. Lecacheux, “Dynamic spectra of some terrestrial ionospheric effects at decametric wavelengths - Applications in other astrophysical contexts,” *Astronomy and Astrophysics*, vol. 96, pp. 296–301, Mar. 1981.
- [10] S. Close, M. Oppenheim, S. Hunt, and L. Dyrud, “Scattering characteristics of high-resolution meteor head echoes detected at multiple frequencies,” *Journal of Geophysical Research: Space Physics*, vol. 107, no. A10, 2002.
- [11] C.-F. Enell, A. Kero, E. Turunen, T. Ulich, P. Verronen, A. Seppälä, S. Marple, F. Honary, A. Senior et al., “Effects of D-region RF heating studied with the Sodankylä Ion Chemistry model,” *Annales Geophysicae*, vol. 23, no. 5, pp. 1575–1583, 2005.
- [12] A. Kero, T. Bösinger, P. Pollari, E. Turunen, and M. Rietveld, “First EISCAT measurement of electron-gas temperature in the artificially heated D-region ionosphere,” *Annales Geophysicae*, vol. 18, no. 9, pp. 1210–1215, 2000.

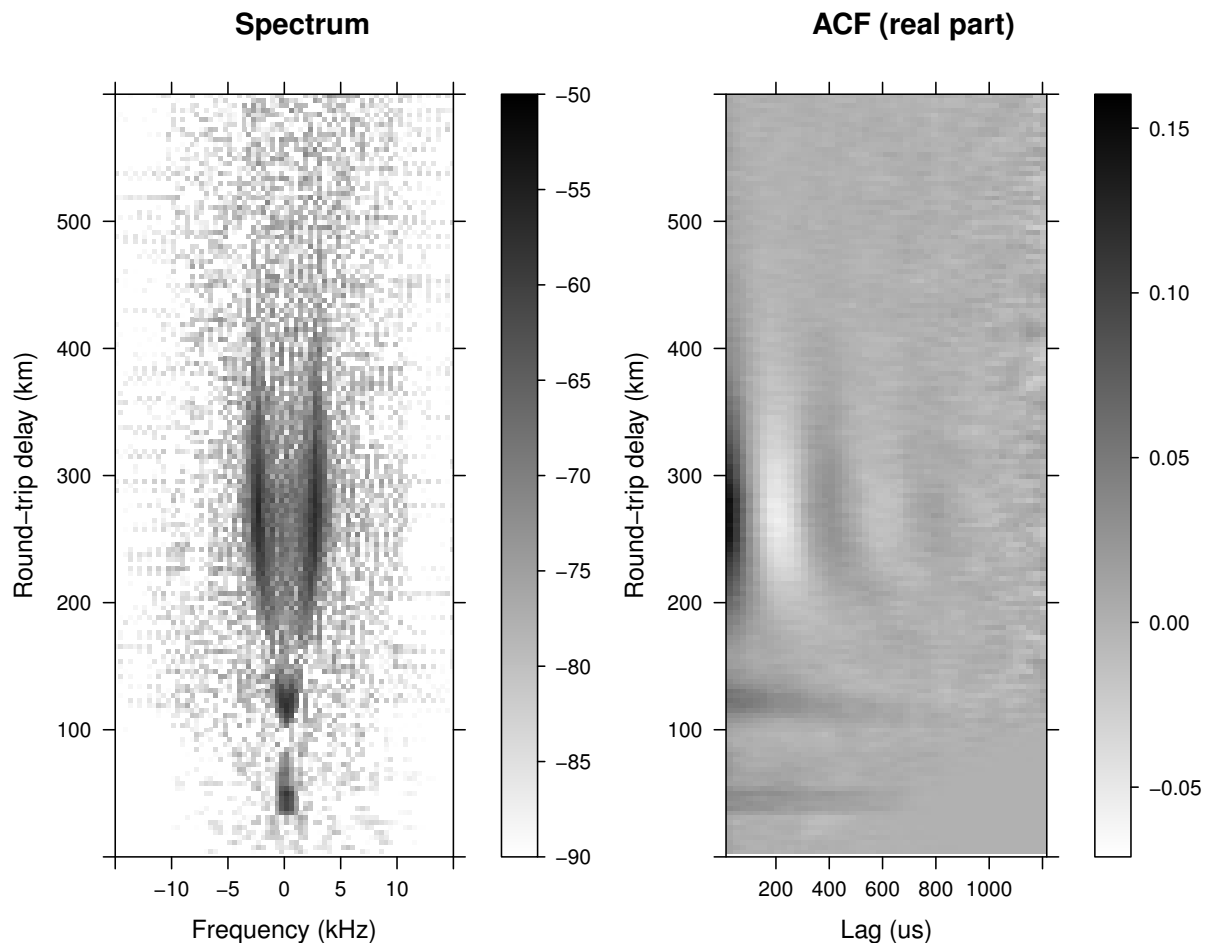


Fig. 2. First multi-beam bi-static incoherent scatter radar measurement demonstrating the measurement of a full ionospheric incoherent scatter spectrum profile. Different altitude regions measured with the different beams are summed together to form a single profile. The spectrum is shown on the left and power is reported in dB units in arbitrary scale. The real part of the autocorrelation function estimates are shown on the right.

- [13] A. Senior, M. T. Rietveld, F. Honary, W. Singer, and M. J. Kosch, "Measurements and modeling of cosmic noise absorption changes due to radio heating of the D region ionosphere," *Journal of Geophysical Research: Space Physics*, vol. 116, no. A4, 2011.
- [14] M. C. Kelley, D. T. Farley, and J. Röttger, "The effect of cluster ions on anomalous VHF backscatter from the summer polar mesosphere," *Geophysical Research Letters*, vol. 14, no. 10, pp. 1031–1034, 1987.
- [15] R. Vondrak, "Incoherent-scatter radar measurements of electric field and plasma in the auroral ionosphere," in *High-Latitude Space Plasma Physics*, ser. Nobel Foundation Symposia Published by Plenum, B. Hultqvist and T. Hagfors, Eds. Springer US, 1983, vol. 54, pp. 73–93.
- [16] M. J. Nicolls, M. P. Sulzer, N. Aponte, R. Seal, R. Nikoukar, and S. A. Gonzalez, "High-resolution electron temperature measurements using the plasma line asymmetry," *Geophysical Research Letters*, vol. 33, no. 18, 2006.
- [17] J. Vierinen, M. S. Lehtinen, M. Orispää, and I. I. Virtanen, "Transmission code optimization method for incoherent scatter radar," *Annales Geophysicae*, vol. 26, no. 9, pp. 2923–2927, 2008.
- [18] I. I. Virtanen, M. S. Lehtinen, T. Nygrén, M. Orispää, and J. Vierinen, "Lag profile inversion method for EISCAT data analysis," *Annales Geophysicae*, vol. 26, no. 3, pp. 571–581, 2008.
- [19] C. G. Little and H. Leinbach, "The Riometer – A Device for the Continuous Measurement of Ionospheric Absorption," *Proceedings of the IRE*, vol. 47, no. 2, pp. 315–320, 1959.
- [20] M. Beharrell and F. Honary, "A new method for deducing the effective collision frequency profile in the d-region," *Journal of Geophysical Research: Space Physics*, vol. 113, no. A5, 2008.
- [21] R. Parthasarathy, G. M. Lerbald, and C. G. Little, "Derivation of electron-density profiles in the lower ionosphere using radio absorption measurements at multiple frequencies," *Journal of Geophysical Research*, vol. 68, no. 12, pp. 3581–3588, 1963.

Measured absorption (dB)

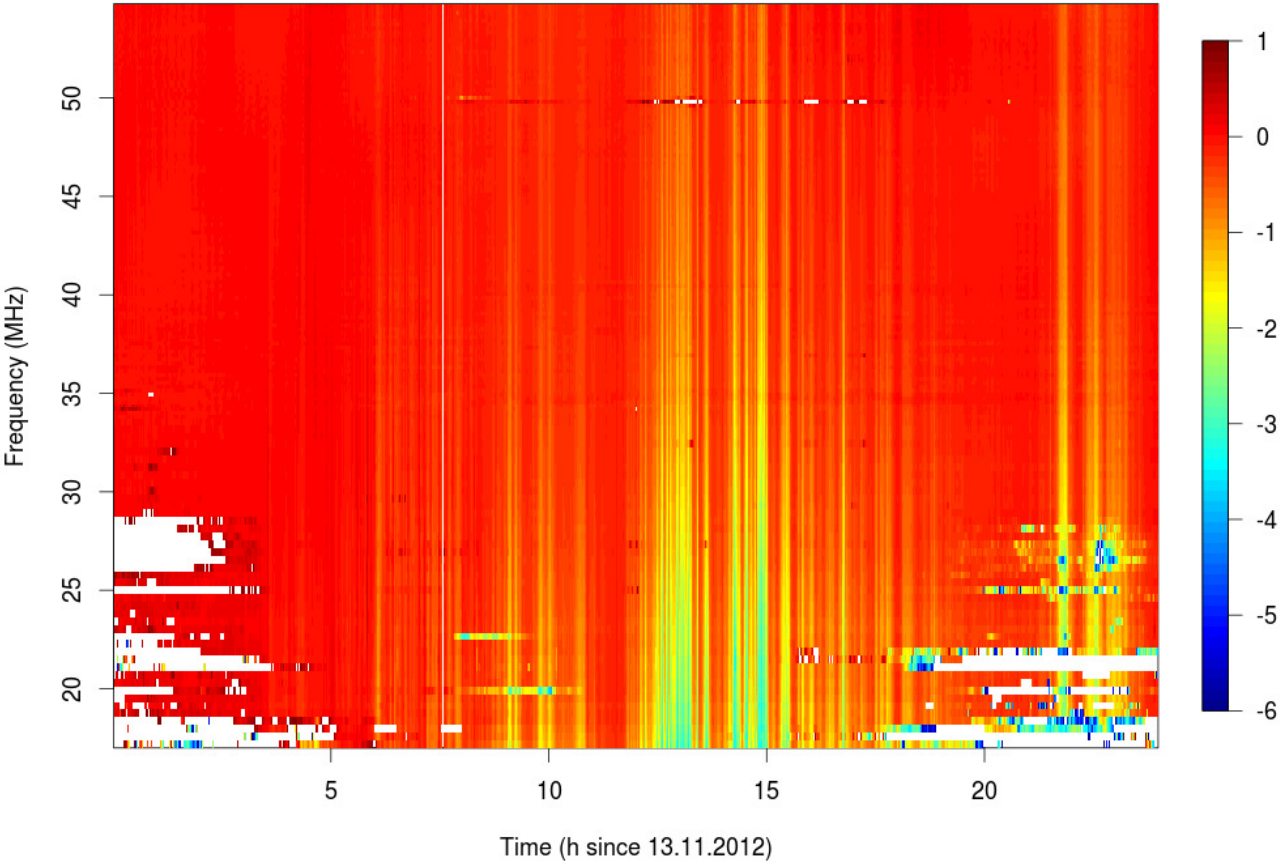


Fig. 3. Measured absorption on the vertical beam of the LBA, starting from 12 UTC on 13 November 2012. The white sections are excised radio-frequency interference.